YALE JOURNAL OF BIOLOGY AND MEDICINE 90 (2017), pp.403-415.

REVIEW

YJBM

Tumor Regulation of Lymph Node Lymphatic Sinus Growth and Lymph Flow in Mice and in Humans

Lauren M. Habenicht[a,b], Sara B. Kirschbaum[c], Momoko Furuya[c], Maria I. Harrell[c,d], and Alanna Ruddell[a,c,e,*]

[a]Department of Comparative Medicine, University of Washington, Seattle, WA; [b]Harvard Center for Comparative Medicine, Harvard Medical School, Boston, MA; [c]Fred Hutchinson Cancer Research Center, Seattle, WA; [d]Department of Obstetrics and Gynecology, University of Washington, Seattle, WA; [e]Department of Comparative Medicine, University of Washington School of Medicine, Seattle, WA

The lymphatic vasculature collects and drains fluid and cells from the periphery through lymph nodes (LNs†) for immune monitoring, and then returns lymph to the bloodstream. During immune responses LNs enlarge and remodel, featuring extensive growth of lymphatic sinuses (lymphangiogenesis). This LN lymphangiogenesis also arises in cancer, and is associated with altered lymph drainage through LNs. Studies of mouse solid tumor models identified lymphatic sinus growth throughout tumor-draining LNs (TDLNs), and increased lymph flow through the expanded sinuses. Mice developing B cell lymphomas also feature LN lymphangiogenesis and increased lymph flow, indicating that these changes occur in lymphoma as well as in solid tumors. These LN alterations may be key to promote tumor growth and metastasis to draining LNs and distant organs. Lymphatic sinus growth within the TDLN may suppress anti-tumor-immune responses, and/or the increased lymph drainage could promote metastasis to draining LNs and distant organs. Investigations of human cancers and lymphomas are now identifying TDLN lymphatic sinus growth and increased lymph flow, that correlate with metastasis and poor prognosis. Pathology assessment of TDLN lymphangiogenesis or noninvasive imaging of tumor lymph drainage thus could potentially be useful to assist with diagnosis and treatment decisions. Moreover, the expanded lymphatic sinuses and increased lymph flow could facilitate vaccine or drug delivery, to manipulate TDLN immune functioning or to treat metastases. The insights obtained thus far should encourage further investigation of the mechanisms and consequences of TDLN lymphatic sinus growth and lymph flow alterations in mouse cancer models, and in human cancer patients.

*To whom all correspondence should be addressed: Alanna Ruddell, Department of Comparative Medicine, University of Washington School of Medicine, 1959 NE Pacific St., Box 357340, Seattle, WA 98195. Phone: 206-685-1216, Fax: 206-685-3006, Email: ruddella@uw.edu.

†Abbreviations: BEC, blood endothelial cell; DMBA/TPA, 7,12-Dimethylbenz[a]anthracene/ 12-*O*-tetradecanoylphorbol-13-acetate; FRC, fibroreticular cell; HEV, high endothelial venule; LEC, lymphatic endothelial cell; LN, lymph node; LV, lymphatic vessel; MRI, magnetic resonance imaging; MHC, major histocompatibility complex; PD-L1, programmed death ligand-1; SMA, smooth muscle actin; TDLN, tumor-draining LN; VEGF, vascular endothelial growth factor; WT, wild-type.

Keywords: tumor-draining lymph node, lymphangiogenesis, lymph flow, cancer, lymphography, lymphatic endothelium

Author Contributions: LH, experimental design, analysis, and writing (NCI R01 CA68328); SK, experimental design and statistical analysis (NCI R01 CA68328); MF, experimental design and analysis (NCI R01 CA68328); MH, experimental design and statistical analysis (NCI R01 CA68328); AR, experimental design, analysis, and writing (grant NCI R01 CA68328 and FHCRC/UW Cancer Consortium Cancer Center Support Grant NIH NCI 5 P30 CA015704).

INTRODUCTION

The lymphatic vasculature serves to drain fluid, molecules, and cells from tissues for return to the blood circulation via thoracic duct delivery of lymph into the pulmonary vein [1,2]. Lymph is first taken up by blind-ended initial lymphatic vessels (LVs) that join to form muscle-coated collecting lymphatic vessels, which connect to a series of draining lymph nodes (LN) as the lymph returns to the heart. Within LNs the lymph is sampled by immune cells including lymphocytes, subcapsular macrophages, and dendritic cells, in order to encounter antigens and generate immune responses [3]. LNs enlarge and undergo extensive remodeling during immune responses to bacterial [4] or viral antigens [5], involving lymphocyte accumulation and proliferation of stromal components including lymphatic endothelial cells (LEC), fibroreticular cells (FRC), and blood endothelial cells (BEC) [6]. Within weeks the LN B cells form germinal centers, while T cells are activated to generate an adaptive immune response. At 5 to 10 days after the initial activation stage LN lymphatic sinus growth becomes prominent, continuing for over a month after infection [7]. Similar hypertrophy, lymphocyte accumulation, and lymphangiogenesis are features of tumor-draining lymph nodes (TDLNs) [8], and of LNs draining arthritic joints in autoimmune disease [9].

While the functional significance of LN lymphangiogenesis is not yet known, it has been proposed to suppress continuation of immune responses that could be deleterious [10,11]. In support of this idea, LN lymphatic endothelium can present antigens in a non-productive manner, to prevent T lymphocyte activation or survival [12-14]. However, it remains to be determined whether the increased LN lymphatic sinuses arising late in infections, or in autoimmune disease do contribute to suppression of immune responses. The expanded LN lymphatic sinus network could additionally promote delivery of antigens to the LN to reinforce peripheral tolerance, and/or to drain accumulated fluid and cell debris generated by inflammation. In cancer, the suppression of self or tumor antigen responses could block TDLN anti-tumor immune responses [15,16], although the requirement for lymphatic sinus growth in this process has not yet been investigated. Nonetheless, studies thus far provide evidence that TDLN lymphatic sinus growth and/or altered lymph drainage may be key to control tumor growth and metastasis. In this review we will discuss the TDLN lymphatic sinus and lymph drainage alterations and consequences that have been identified thus far in mouse models of cancer, and will compare these findings with reports of similar TDLN alterations in humans with cancer.

TOPICS

Lymph Node Lymphatic Sinus Growth in Murine Cancers

Naïve murine lymph nodes from young wild-type (WT) mice in specific pathogen-free animal facilities exhibit sparse lymphatic sinuses arranged around the outer margins of the cortex and medulla [17]. The medulla and cortex each comprise roughly half of the LN, surrounding the central T cell paracortex, as illustrated in Figure 1a. In normal 6 week-old mice, the subcapsular purple-staining lymphatic sinus surrounding the cortex of normal young mice is thin (Figure 1b; arrow), and cortical sinuses are not detected. In contrast, the medullary lymphatic sinuses are more developed (Figure 1b; arrowhead). Afferent lymphatic vessels (LVs) deliver lymph into the subcapsular and cortical sinuses, and then into the medullary sinuses that drain lymph to the efferent LV. As the immune system matures the lymphatic sinus network becomes more prominent, and mice develop primary B cell follicles and germinal centers in the cortex, while the medulla and paracortex mainly harbor T lymphocytes.

LN lymphatic sinus growth (lymphangiogenesis) has now been identified in the TDLNs of a variety of mouse models of cancer (Table 1). Both the cortical and medullary sinuses can grow and extend centrally into the B and T cell regions, respectively [18,19]. These changes are restricted to the TDLN but not non-draining LNs, indicating that they are induced by tumor lymph drainage [18]. TDLN lymphatic sinus growth has been identified in mice bearing melanoma or nasopharyneal carcinoma cell line implants in the footpad that drain to the popliteal LN [18,19]. In lung carcinoma cell line implants in the flank, lymphangiogenesis is induced in draining and non-draining inguinal and axillary LNs [20]. Polyoma middle T antigen transgenic mice developing metastatic mammary carcinoma also developed generalized LN lymphangiogenesis [20]. Squamous cell carcinomas induced by DMBA chemical mutagenesis and TPA tumor promotion caused extensive LN lymphangiogenesis [21]. Lymphatic sinus growth throughout LNs was also detected in young preneoplastic E-μ-*c-myc* mice (Figure 1c), even before the generation of metastatic B cell lymphomas [22]. In these mice, B lymphocyte accumulation throughout the LN drives extensive lymphatic sinus growth, so that the cortex and medulla cannot be distinguished (Figure 1c). These examples demonstrate that LN lymphangiogenesis is a feature of both solid tumors and lymphomas at early stages of tumor formation.

The development of LN lymphangiogenesis consistently preceded detection of tumor metastasis to the TDLN in solid tumor models (Table 1). Sensitive PCR assays did not identify melanoma cells in TDLNs exhibiting lymphangiogenesis [23], suggesting that these changes are me-

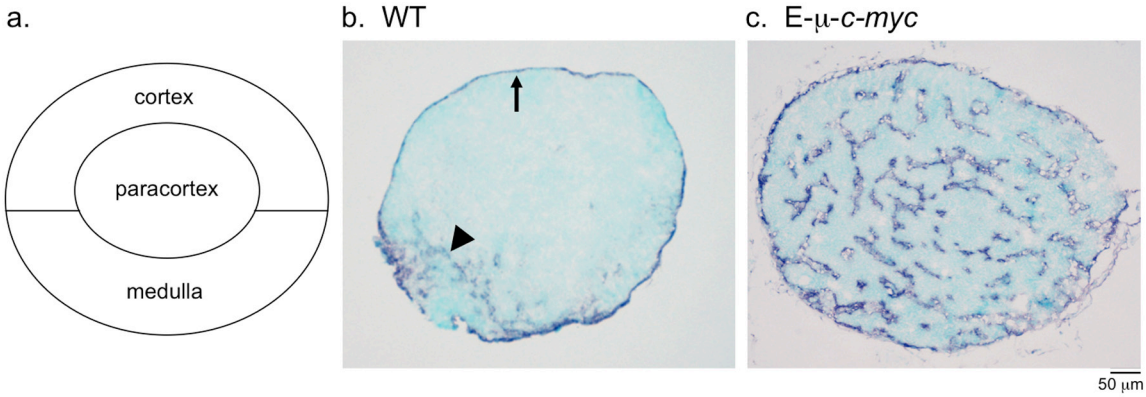

Figure 1. Lymph node lymphatic sinus growth in E-μ-*c-myc* mice. a). Schematic of lymph node gross anatomy, illustrating the location of the cortex that contains thin subcapsular and cortical lymphatic sinuses and B lymphocytes, the paracortex containing conduits and T lymphocytes, and the medulla containing medullary lymphatic sinuses and T lymphocytes. **b**). Immunostaining with LYVE-1 antibody demonstrates subcapsular (arrow) and medullary (arrowhead) purple-stained lymphatic sinuses in popliteal LN of normal 6 week-old WT C57Bl6/J mouse, with Methyl Green nuclear counterstaining. **c**). LYVE-1 immunostaining identifies extensive lymphatic sinus growth throughout the LN from a preneoplastic 6 week-old E-μ-*c-myc* mouse, so that the cortex and medulla cannot be distinguished. Scale bar 50 μm.

diated by tumor antigens or signals rather than by delivery of tumor cells into the LN. Outbred mice developing benign papillomas after DMBA/TPA carcinogen and tumor promoter treatment showed modest TDLN lymphangiogenesis, while mice whose lesions transformed to form invasive and metastatic carcinomas exhibited much more extensive lymphatic sinus growth [21]. In addition, p19 Arf- or p53-tumor suppressor-deficient mice that rapidly progress to form invasive carcinomas exhibited extensive lymphangiogenesis at the benign papilloma stage, before conversion to invasive and metastatic carcinomas. VEGF-A- [24] or VEGF-C-overexpressing mice [25] developing DMBA/TPA-induced carcinomas also exhibited growth of tumor LVs and LN lymphatic sinuses, which were also associated with increased metastasis to LNs. VEGF-C treatment also promoted LN lymphatic sinus growth and metastasis of Lewis Lung Carcinoma cell line implants [20]. Taken together, these findings suggest that LN lymphatic sinus growth precedes and predicts the generation of metastatic tumors.

Lymph Node Lymphatic Endothelial Modulation of Adaptive Immune Responses

LN lymphatic endothelial cells (LEC) can generate and present a variety of peripheral tissue antigens via major histocompatibility complex (MHC) class I, and this has been proposed to reinforce peripheral immune tolerance [12,26]. These LEC do not express co-stimulatory molecules such as CD80/86 required for T cell activation, while they do express inhibitory ligands such as programmed death ligand-1 (PD-L1) so that engaged CD8 lymphocytes may instead be suppressed or deleted [3,16,27]. LN LEC can also cross-present tumor antigens obtained from the lymph [13,28] or from dendritic cells [29] on MHC class II to promote CD4 suppression [30]. LN LEC can additionally produce immunosuppressive molecules such as nitric oxide *in vitro*, which could also promote a tolerant microenvironment within the LN [31,32]. The fibroreticular cells (FRC) that coat conduit fibers within LNs [33,34] also present subsets of peripheral tissue antigens [26], and contribute nonproductive antigen presentation and nitric oxide production *in vitro* [31]. These and other studies suggest that the TDLN LEC (and FRC) can promote the generation of an immunosuppressive environment [16,35,36]. However, the effects of TDLN remodeling and of lymphangiogenesis on T and B lymphocyte immune responses have not yet been investigated *in vivo.* The consequences for LN responses to lymph-derived tumor antigens versus self antigens also remain to be distinguished *in vivo.*

B Lymphocyte Regulation of Tumor-draining Lymph Node Lymphatic Sinus Growth

B lymphocytes appear to be key for generation of LN lymphangiogenesis during immune responses [4,5,10]. In E-μ-*c-myc* transgenic mice, accumulation and spread of c-Myc-expressing B cells through the LNs of young preneoplastic mice [22] is associated with rapid lymphatic sinus growth throughout the LNs, so that the normal cortical and medullary anatomy is obscured (Figure 1c). Accumulation of B cells is required for lymphatic sinus growth in TDLNs of wild-type (WT) mice developing

Table 1. Examples of lymph node lymphangiogenesis in mouse models of cancer.

Cancer	Method of Tumor Induction	Key Findings	Reference
B cell lymphoma	E-μ-*c-myc* transgenic mouse	LN lymphangiogenesis increases lymph flow and precedes generation of metastatic lymphoma	[22]
Lung Carcinoma	Lewis lung carcinoma cell line	LN lymphangiogenesis precedes metastasis	[20]
Mammary Carcinoma	Polyoma middle T antigen transgenic mouse	LN lymphangiogenesis precedes metastasis	[20]
Melanoma	B16-F10 cell line	B cells drive TDLN lymphangiogenesis and increase lymph flow before metastasis	[18]
Nasopharyngeal carcinoma	CNE-2 cell line	Tumors induce TDLN lymphangiogenesis	[19]
Squamous cell carcinoma	DMBA-TPA-induced	B cell accumulation and LN lymphangiogenesis precede and predict invasive carcinoma	[21]
Squamous cell carcinoma Expressing VEGF-A	DMBA-TPA-induced	Tumor VEGF-A overexpression increases LN lymphangiogenesisbefore and after metastasis	[24]
Squamous cell carcinoma expressing VEGF-C	DMBA-TPA-induced	Tumor VEGF-C overexpression increases LN lymphangiogenesis and increases metastasis	[25]

B16-F10 melanoma, as TDLN lymphatic sinuses fail to grow in B cell-deficient mice [18]. Interestingly, in the DMBA/TPA squamous cell carcinoma model, the extent of B cell accumulation predicts the extent of TDLN lymphangiogenesis, and also the potential to form invasive and metastatic carcinomas [21]. These findings suggest that B lymphocytes are a critical determinant of TDLN lymphangiogenesis and of metastasis. In support of this idea, implantation of melanoma and lymphoma cells into preneoplastic E-μ-*c-myc* mice featuring B lymphocyte accumulation and LN lymphangiogenesis greatly increased metastasis via the lymphatics to draining LNs, and then through the bloodstream to distant organs [23]. Tumor growth also modestly increased in these short-term tumor models. The effects of B lymphocytes on tumor growth and metastasis could involve downstream effects of the lymphatic sinus growth in E-μ-*c-myc* mice to promote immune tolerance, although this question has not yet been investigated. One study thus far has reported that introduced T lymphocytes inhibit LN lymphatic sinus growth after introduction into T cell-deficient nude mice [37]. It remains to be determined how B and T lymphocytes coordinate the extensive lymphangiogenesis that is observed in the B cell cortex and also in the T cell paracortex during immune responses [10] or in TDLNs [38].

Taken together, the studies thus far suggest that B lymphocytes are required to drive TDLN lymphangiogenesis [18], and that the growth of these lymphatic sinuses predicts tumor metastatic potential (Table 1) preceding significant metastasis to LNs [23]. Moreover, LNs featuring lymphangiogenesis promote growth and metastasis of lymphomas and melanomas to draining LNs and distant organs [23]. These findings suggest the hypothesis that TDLN lymphatic sinus growth actively promotes tumor dissemination, so that lymphangiogenesis could provide a critical target for therapeutic intervention to block metastasis. Further studies are required to directly test and identify the role of LN lymphangiogenesis in tumor dissemination. As LN LEC have been proposed to suppress anti-tumor immune responses [15,27], it will be particularly interesting to determine the effect of TDLN lymphatic sinus growth on the anti-tumor immune response.

Molecules Regulating Lymph Node Lymphatic Sinus Growth

A number of factors have been identified that can promote the growth of LVs, and the best characterized include vascular endothelial growth factor (VEGF)-A, -C, and -D [39,40]. It has been difficult to study the direct effects of lymphatic growth factors on TDLN lymphatic sinuses, as these same growth factors can also promote tumor-associated LV growth. Moreover, VEGF-A promotes growth of the tumor blood vasculature, which

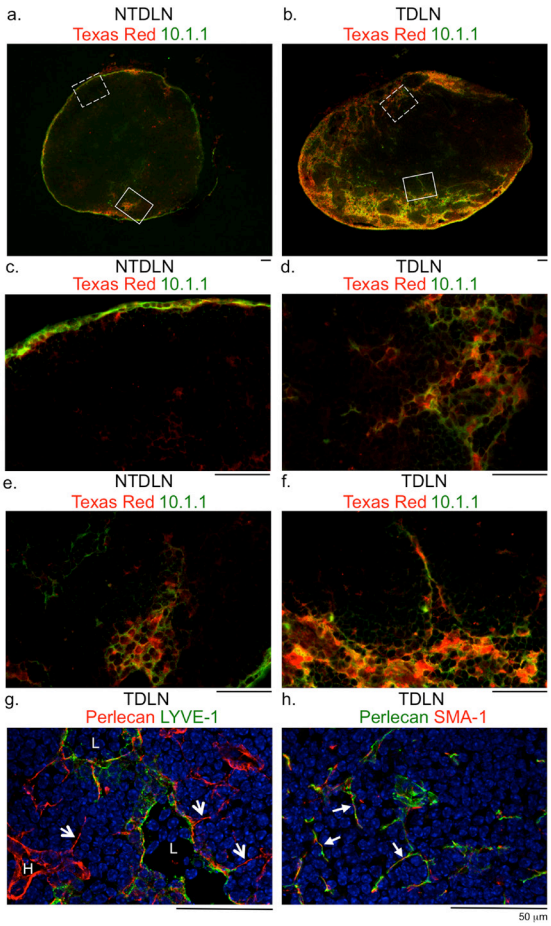

Figure 2. Lymph drainage through lymphatic sinuses of tumor-draining lymph nodes. B16-F10 tumors were injected in one rear footpad of 5-week-old C57Bl/6J mice and grown for 3 weeks. Some mice (panels **a**-**f**) were anesthetized and injected in both dorsal toes with Texas Red dextran (Lysine-fixable 10,000 MW) to label the popliteal LN lymph drainage for 20 min before euthanasia (n = 9), while other mice were not injected with dextran (panels **g**,**h**). The lymphatic sinuses of the draining popliteal LNs were examined by immunostaining paraformaldehyde-fixed cryosections with 10.1.1 antibody (green). A small amount of Texas Red dextran is confined to the green lymphatic sinuses in the NTDLN (**a**). In the TDLN, much larger amounts of dextran are identified in the expanded green lymphatic sinuses (**b**). The white dashed boxes outline cortical regions shown at higher magnification in (**c**) and (**d**), while the outlined solid white boxes outline medullary regions shown at higher magnification in (**e**) and (**f**). Texas Red dextran is largely confined to the subcapsular and cortical lymphatic sinuses of the NTDLN (**c**) and TDLN (**d**). In the medulla, Texas Red dextran is largely confined to the sinuses, and is greatly increased in TDLNs (**f**), relative to the NTDLN (**e**). Red perlecan and green LYVE-1 lymphatic sinus immunostaining and Deltavision microscope imaging (Applied Biosciences) of the paracortex region adjacent to the medulla (**g**) identifies perlecan fibers surrounding lymphatic sinuses (L), high endothelial venules (H), capillaries, and conduits (arrows). Green perlecan immunostaining in combination with red SMA-1 immunostaining of FRCs (**h**) identifies the conduits of the paracortex (arrows). Scale bars for each image are 50 μm.

is required for tumor growth [41]. Nonetheless, evidence has been obtained that forced B cell expression of VEGF-A promotes LN lymphatic sinus growth [42], and c-Myc-expressing B cells express increased VEGF-A that is associated with LN lymphangiogenesis in E-μ-*c-myc* mice [22]. Tumor VEGF-A [24] or VEGF-C expression at high levels [25] both promote tumor-draining LV and LN lymphatic sinus growth. Erythropoietin treatment [43] or cyclooxygenase-2 production of prostaglandin E_2 [44] can also induce LN lymphangiogenesis and promote tumor metastasis. An mCLCA1 LEC surface protein has been found to promote rapid lymphatic sinus growth that may be induced by lymphocyte LFA-1 binding to mCLCA1 [45,46], so that LN lymphatic sinus growth may be influenced by multiple pathways. Further studies will also be required to identify the critical regulators of TDLN lymphangiogenesis, and to determine whether these factors act through direct effects on the lymphatic sinus-

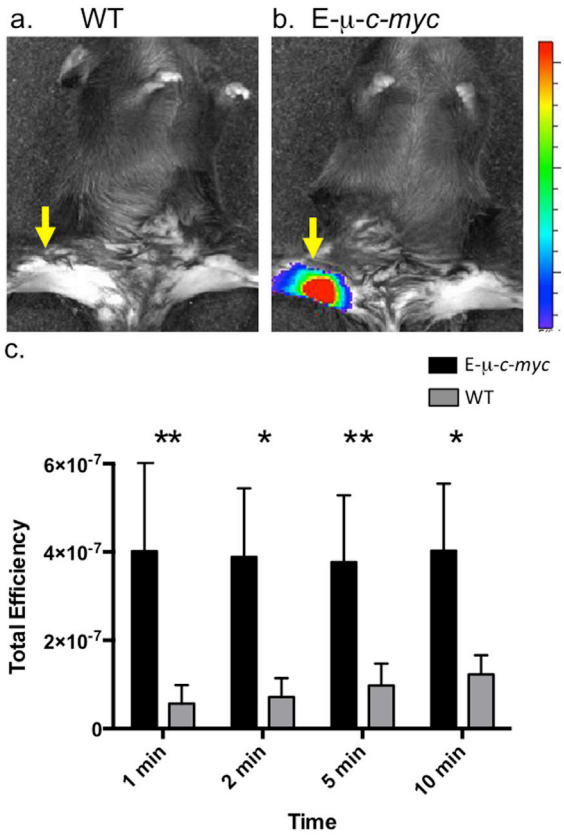

Figure 3. Lymph node lymph flow increases in reneoplastic E-μ-*c-myc* mice. Near infrared imaging of 52 nm diameter quantum dots (800 nm emission, Invitrogen) using a Xenogen IVIS CCD camera, 10 min after injecting 25 microliters of quantum dots into the dorsal rear toe of the right leg of 6-week-old WT (**a**) or E-μ-*c-myc* mouse (**b**), draining to the popliteal LN (arrows). **c**). Total fluorescence efficiency was measured in a region of interest drawn over the popliteal LN of each mouse and pre-injection fluorescence efficiency of the same region of interest was subtracted at each time point. Standard errors are shown. Differences between WT and E-μ-*c-myc* mice at each time point are statistically significant by Mann-Whitney test (N = 10; *, $p < 0.05$; **, $p < 0.01$).

es, and/or by indirect effects from modulation of tumor lymphangiogenesis, angiogenesis, or lymph drainage.

Imaging Lymph Drainage Through Lymph Nodes

The lymphatic circulation can be mapped by subcutaneous injection of India Ink [47], as these carbon nanoparticles of 20 to 70 nm diameter are taken up by LNs within minutes [48,49]. In fact, initial lymphatic vessels readily acquire molecules up to 70 nm diameter from the interstitium after subcutaneous injection [50-52]. Similarly, LNs rapidly filter the lymph upon entry to the subcapsular lymphatic sinuses, retaining molecules larger than ~40 to 70 kD while allowing smaller molecules to enter the conduits, as detected by microscopy of LN sections obtained from mice subcutaneously injected with these tracers [49,53] or by intravital microscopy *in vivo* [54,55]. Lymph drainage can also be visualized *in vivo* at lower resolution, using digital video cameras to grossly detect uptake of near infrared dyes such as indocyanine green [56,57] or near infrared nanoparticles [18,58] through LVs and LNs.

Magnetic resonance imaging (MRI) using low molecular weight gadolinium [59] or nanoparticle-based gadolinium contrast [60,61] has been useful to provide high resolution images of lymph drainage through LVs and LNs of anesthetized mice. The LN lymphatic sinuses themselves have been indirectly visualized *in vivo* by optical imaging using fluorescent LYVE-1 antibody [62] or lymphatic sinus-binding LyP-1 peptide [63], although the images are of low resolution. Positron emission tomography using radio-labelled LYVE-1 antibody can also be to obtain low resolution images to measure LN lymphatic sinus content *in vivo* [64]. In human cancer patients, lymphoscintigraphy using radioactive sulfur colloidal nanoparticles and visible Isosulfan Blue dye is commonly used for low resolution imaging of lymph drainage to identify the first (sentinel) TDLN, for biopsy and pathology analysis of LN metastasis [65,66].

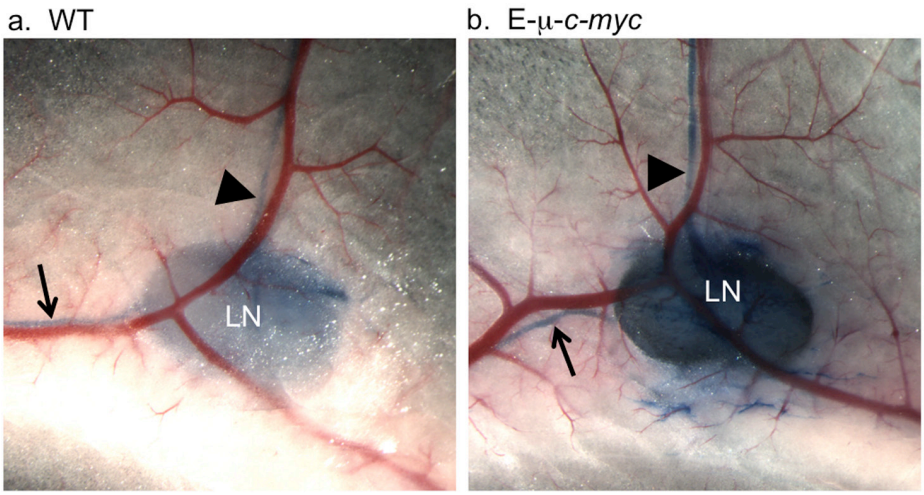

Figure 4. Collecting lymphatic vessels show similar morphology in wild-type and E-μ-*c-myc* mice. Anesthetized 6-week-old WT (**a**) and E-μ-*c-myc* mice (**b**) were injected with 5% Evans Blue dye (80 μl) in the tailbase and in the rear dorsal toe (Sigma), followed by euthanasia 30 minutes later. The skin of the flank was reflected from the body wall, placed flat, and photographed in a stereomicroscope. The arrows indicate the afferent LV from the gluteal LN to the inguinal LN. The arrowheads indicate the efferent LV that travels along the milk line from the inguinal LN to the axillary LNs. While much more Evans Blue is taken up in E-μ-*c-myc* mice, the morphology of the afferent and efferent LVs is similar.

Increased Lymph Flow Through Tumor-draining Lymph Nodes

Mice bearing B16-F10 footpad melanoma tumors have been useful to compare tumor-induced lymph flow through the TDLN versus the uninvolved contralateral popliteal NTDLN within the same mouse [18]. Injection of small numbers of melanoma cells into the footpad generate small tumors of 3 to 7 mm diameter that grow slowly and do not inhibit locomotion or visibly affect mouse behavior through about 21 days [18]. Xenogen IVIS imaging of 52 nm diameter near infrared quantum dots (800 nm; Invitrogen) injected into the dorsal toes of anesthetized mice identified greatly increased lymph flow through the TDLN, and very little drainage in the NTDLN [18]. Fluorescence microscopy determined that the extensive growth of lymphatic sinuses mediates this increased lymph delivery to TDLNs [67], as illustrated by injection of fluorescent dextran (10,000 MW lysine-fixable Texas Red dextran, Sigma) into both dorsal toes of mice bearing B16-F10 melanoma in one rear footpad before euthanasia and immunostaining of LN cryosections (Figure 2). Nearly all of the Texas Red dextran was confined to the 10.1.1 Ab-stained cortical and medullary lymphatic sinuses (Figure 2a). Even with the greatly increased dextran uptake in TDLNs, the majority of lymph was confined to the lymphatic sinuses for at least 20 min after injection (Figure 2b). This is also evident in high magnification images of the LN parenchyma adjacent to the cortical and medullary sinuses of NTDLNs (Figure 2c, e) and of TDLNs (Figure 2d, f).

Some of the lymph in LN lymphatic sinuses enters tiny conduits in the B and T cell regions that connect to HEVs [49,68]. These conduits deliver antigens to dendritic cells coating the conduits, and to lymphocytes associated with HEVs [54,55]. Interestingly, the lymphatic sinuses filter lymph before entry to the conduits, as only molecules smaller than ~40 to 70 kD can be detected within the conduits [49,53]. The conduits are distributed throughout the parenchyma of LNs [49], and they can be identified at high magnification by immunostaining for the perlecan matrix component (arrows, Figure 2g). Perlecan also coats the much larger lymphatic sinuses (Figure 2g; L) and HEVs (Figure 2g; H) [55]. The conduits are coated with FRC that express smooth muscle actin (SMA) [55], as illustrated by perlecan/SMA immunostaining in Figure 2h (arrows). While low molecular weight dextran within conduits can be weakly detected in the LN parenchyma within 20 min after injection [49,55], we were unable to detect much if any fluorescent dye in the conduits or in the parenchyma adjacent to the cortical (Figure 2c, e) or medullary (Figure 2d, f) lymphatic sinuses in LN cryosections at 20 min after injection, even in TDLNs where LN lymph drainage was greatly increased. Dextran is also largely confined to the lymphatic sinuses of cryosections from normal or inflamed LNs harvested 5 min after injection [49]. Intravital microscopy of normal LNs of anesthetized mice identified transient transport of lymph-derived dextran through the conduits within the first min after injection, with the bulk of the injected dextran entering and persisting within the

Table 2. Examples of lymph node lymphangiogenesis in human cancers.

Cancer	Key Findings	Reference
Breast cancer	Lymphangiogenesis is increased in metastatic TDLNs	[100]
Breast cancer	TDLN lymphangiogenesis predicts non-TDLN metastasis	[101]
Lymphoma	Lymphangiogenesis in lymphoma LNs	[93]
Melanoma	Lymphangiogenesis in metastatic lymph nodes is associated with distant metastasis	[102]
Oral squamous cell carcinoma	TDLN lymphangiogenesis precedes metastasis	[103]
Oral squamous cell carcinoma	TDLN lymphangiogenesis predicts LN metastasis	[104]
Rectal Carcinoma	TDLN lymphangiogenesis predicts poor prognosis	[105]

lymphatic sinuses over time [54,55]. Thus, while the conduit lymph drainage may facilitate local antigen presentation to lymphocytes and dendritic cells in the B and T cell regions [54,55], the conduits do not appear to physically contribute much lymph drainage relative to the large increase in lymphatic sinus lymph delivery into TDLNs.

Increased Lymph Drainage in Lymphoma

E-μ-*c-myc* transgenic mice exhibit LN hypertrophy [69] featuring B cell accumulation and extensive lymphatic sinus growth throughout the LNs (Figure 1c) at early preneoplastic stages, before the formation of metastatic B cell lymphomas [22]. LNs from these mice also exhibit increased lymph drainage through the lymphatic sinuses, as determined by subcutaneous TRITC dextran injection and imaging cryosections of the draining popliteal LNs after euthanasia [22]. This increased LN lymph flow was confirmed using Xenogen IVIS optical imaging after subcutaneous injection of near infrared quantum dots into the rear dorsal toes of anesthetized WT (Figure 3a) and E-μ-*c-myc* mice (Figure 3b). Measurement of the quantum dot uptake in the popliteal LN identified a six-fold increase in E-μ-*c-myc* mice within a minute after injection and continuing over 10 minutes, which was statistically significant (Figure 3c). The mechanism increasing lymph flow into the LNs of E-μ-*c-myc* mice remains to be determined. The afferent (arrows) and efferent (arrowheads) lymphatic vessels of WT (Figure 4a) and E-μ-*c-myc* littermates (Figure 4b) are of similar size and morphology, as illustrated by Evan's Blue dye injection [70] and photography of the inguinal fatpad in necropsies, except that there is much more dye uptake in the LVs and LN of E-μ-*c-myc* mice (Figure 4b). This increased lymph drainage is also not associated with growth of LVs in the injected foot [23]. However, E-μ-*c-myc* B cell c-Myc overexpression within the LNs has multiple effects on transcription and translation [71] that could potentially influence lymphatic functions, such as VEGF-A production [72].

Our findings that the major changes in the vasculature of E-μ-*c-myc* mice involve lymphatic sinus growth throughout the enlarged LNs (Figure 1c), while the afferent and efferent LVs appear normal (Figure 4b), suggest that the LN lymphatic sinus growth itself could promote increased lymph drainage into and through the LNs [22]. For example, the growth of LN lymphatic sinuses could provide a passive sink mechanism to increase lymph flow, where the reduced resistance due to the increased LN sinus area facilitates increased lymph drainage. The LN SMA-positive stromal cells could theoretically provide contractile activity [73] regulated by innervation [74], as contraction has been identified in LN capsules of innervated sheep [75] and cow LNs *ex vivo* [76]. Alternatively, an active mechanism could increase lymph flow via effects on the afferent and efferent LVs, for example by modulating their contraction or dilation, as has been identified in some tumor models [77,78]. The behavior of afferent and efferent LVs at their junction with the LN have not yet been examined by high resolution intravital microscopy of normal or of E-μ-*c-myc* mice. Much remains to be learned about the mechanisms regulating lymph flow through LNs, whether it involves passive or active control by the LNs and/or by LVs entering and leaving the LN.

Lymphography of Tumor-draining Lymph Node Lymph Drainage

MRI has been used to characterize TDLN lymph drainage at higher resolution [79,80]. Dynamic contrast-enhanced imaging after subcutaneous injection of gadolinium contrast into the dorsal toes of mice developing melanoma tumors in one footpad identified increased lymph drainage through the TDLN [81]. Interestingly, this increased lymph drainage could subsequently be detected after delivery from the lymphatic vessels into the bloodstream [81]. These findings suggest that measurement of the appearance of tumor-associated lymph-borne agents in the bloodstream [82] could be used as a surrogate marker of tumor-induced lymph flow. High resolution MRI determined that the injected gadolinium

contrast is largely confined to the cortical margins of normal LNs [67], where the sinuses are transporting lymph (Figure 2a). Interestingly, TDLNs showed strong gadolinium contrast uptake into the medullary sinuses [67], which likely reflects the increased lymph flow through the expanded medullary lymphatic sinuses (Figure 2b). This increased contrast uptake in the medullary sinuses could also make a useful biomarker for non-invasive imaging of TDLN lymphangiogenesis and increased lymph flow, as medullary sinus lymphangiogenesis is a common feature of TDLNs [83].

One caveat of the use of lymphography to map lymph drainage to TDLNs is that murine tumors can sometimes block or divert lymph drainage. Aggressive tumor growth requires rapid formation of an abnormal blood vasculature that includes LVs [84]. High tumor interstitial pressure can divert or block lymph drainage through peritumoral LVs [85,86], and metastasis to LNs can also block lymph drainage [87,88]. Diverted or blocked lymph drainage is also sometimes observed in human cancer patients [85], which complicates the use of lymphography to correctly identify the sentinel or first tumor-draining LN [89,90].

Tumor-draining Lymph Node Lymphangiogenesis and Increased Lymph Flow in Human Cancers

These initial findings from studies of mouse cancer models support a key role of TDLN lymphatic sinus growth, and possibly also of increased lymph drainage, in regulation of tumor growth and metastasis. Investigations in human cancers have identified similar TDLN alterations. The lymphatic vasculature of human LNs is somewhat distinct from that of rodent LNs [91], with a thicker capsule surrounding the human cortical (marginal) and medullary sinuses [92]. The lymphatic vasculature of normal versus tumor-draining human or murine LNs has not been investigated much, so that it is difficult to predict how their structure and lymph drainage functions compare. Nonetheless, TDLN lymphatic sinus growth has recently been identified in several types of human cancers, including melanoma and breast, oral, and rectal cancers (Table 2). Interestingly, the growth of TDLN lymphatic sinuses correlates with poor prognosis and metastasis in several types of cancer (Table 2). Further investigation of TDLN lymphatic sinus growth characteristics could identify additional criteria for cancer diagnosis. LN lymphangiogenesis is also not restricted to solid tumors in humans, as lymphatic sinus growth has been identified in human non-Hodgkins lymphomas [93].

A few studies have assessed lymph drainage in human cancer patients, using lymphoscintigraphy of subcutaneously injected radiolabelled colloidal nanoparticles. In melanomas [94] and other skin cancers [95] increased lymph flow predicted metastasis in SLNs, suggesting that this parameter could be developed to identify those patients with poor prognosis cancers. These findings suggest that noninvasive imaging to identify changes in tumor lymph drainage could improve diagnosis of metastatic potential.

CONCLUSIONS AND OUTLOOK

Studies of TDLNs in mice developing several types of solid tumors or lymphoma identified extensive growth of lymphatic sinuses, which may predict those cancers with metastatic potential. The correlation of TDLN lymphangiogenesis with metastatic potential also suggests that these processes are linked. Observations in a variety of models together provide support for the hypothesis that TDLN lymphatic sinus growth is an essential step in tumor progression to metastasis. [20,23-25]. However, thus far the cells and molecules regulating these processes are not much understood, other than the requirement for B lymphocytes to induce LN lymphatic sinus growth in some models [18,22]. Identification of the mechanisms controlling TDLN lymphangiogenesis will allow direct testing of lymphatic sinus contributions to tumor dissemination.

TDLN hypertrophy and increased lymph flow are characteristic of aggressive tumors, although tumors sometimes can divert or block lymph drainage, particularly after LN metastasis [87,88]. Increased lymph drainage through the expanded medullary sinuses also may be a characteristic of TDLNs, although this has only been demonstrated thus far for murine lymphomas and melanomas [22,67]. Our studies of E-μ-*c-myc* mice suggest that LN lymphatic sinus growth could directly or indirectly contribute to changes in lymph drainage, by active or passive mechanisms that remain to be identified. The increased lymphatic sinuses in TDLNs could potentially enhance the reinforcement of peripheral tolerance, to suppress anti-tumor immune responses [16]. The increased lymph drainage through the expanded lymphatic sinuses could alternatively promote tumor immune suppression by increasing the interaction of lymphocytes with lymph-derived self and tumor antigens, or by influencing flow-regulated immune cell functions [96]. The increased lymph flow could also physically promote spread of tumor cells to the draining LN and distant organs, to facilitate metastasis. Therapies targeting TDLN lymphangiogenesis and lymph drainage could potentially be developed to impose an anti-tumor TDLN microenvironment to inhibit tumor growth at a distance, and/or to prevent tumor dissemination to TDLNs and distant organs. Finally, the ability of TDLNs to concentrate nanoparticles [49,51] suggests that subcutaneous nanoparticle delivery could be particularly useful to target the first TDLN for vaccination or drug treatment [97,98].

The initial findings from human cancers suggest

that pathology analysis of lymphatic sinuses of TDLNs could provide useful diagnostic assays to identify those cancers at risk of metastasis that could require more aggressive treatment. MRI lymphography analysis of lymph flow through TDLNs shows promise to provide a noninvasive approach to assess the metastatic potential of tumors, in addition to identifying TDLN micrometastases [79,80,99]. Detailed studies of larger patient cohorts will establish whether particular changes in structure and function of the lymphatic sinuses of human TDLNs versus uninvolved LNs will be useful for diagnosis and treatment decisions. Comparison of different types of human cancers will also be required to establish whether these TDLN alterations identify metastatic potential in only some tumor types, or if they are more universally predictive for cancer diagnosis. Going forward, comparative studies of murine and human TDLN sinus structure and function should help to identify the critical alterations regulating tumor growth and metastasis.

Acknowledgments: We thank Bryan Turnbull, Kendra Byrd, and Monica Montgomery for their assistance.

REFERENCES

1. Alitalo K, Carmeliet P. Molecular mechanisms of lymphangiogenesis in health and disease. Cancer Cell. 2002;1(3):219-27.
2. Swartz MA. The physiology of the lymphatic system. Advanced Drug Delivery Reviews. 2001;50:3-20.
3. Card CM, Yu SS, Swartz MA. Emerging roles of lymphatic endothelium in regulating adaptive immunity. Journal of Clinical Investigation. 2014;124(3):943-52.
4. Angeli V, Ginhoux F, Llodra J, Quemeneur L, Frenette PS, Skobe M, et al. B cell-driven lymphangiogenesis in inflamed lymph nodes enhances dendritic cell mobilization. Immunity. 2006;24:203-15.
5. Kumar V, Scandella E, Danuser R, Onder L, Nitschke M, Fukui Y, et al. Global lymphoid tissue remodeling during a viral infection is orchestrated by a B cell-lymphotoxin-dependent pathway. Blood. 2010;115(23):4725-33.
6. Chyou S, Benahmed F, Chen J, Kumar V, Tian S, Lipp M, et al. Coordinated regulation of lymph node vascular-stromal growth first by CD11c+ cells and then by T and B cells. J Immunol. 2011;187(11):5558-67.
7. Tan KW, Yeo KP, Wong FH, Lim HY, Khoo KL, Abastado JP, et al. Expansion of cortical and medullary sinuses restrains lymph node hypertrophy during prolonged inflammation. J Immunol. 2012;188(8):4065-80.
8. Ji RC. Lymph node lymphangiogenesis: a new concept for modulating tumor metastasis and inflammatory process. Histol Histopathol. 2009;24(3):377-84.
9. Guo R, Zhou Q, Proulx ST, Wood R, Ji RC, Ritchlin CT, et al. Inhibition of lymphangiogenesis and lymphatic drainage via vascular endothelial growth factor receptor 3 blockade increases the severity of inflammation in a mouse model of chronic inflammatory arthritis. Arthritis Rheum. 2009;60(9):2666-76.
10. Liao S, Ruddle NH. Synchrony of high endothelial venules and lymphatic vessels revealed by immunization. J Immunol. 2006;177(5):3369-79.
11. Tan KW, Chong SZ, Angeli V. Inflammatory lymphangiogenesis: cellular mediators and functional implications. Angiogenesis. 2014;17(2):373-81.
12. Cohen JN, Guidi CJ, Tewalt EF, Qiao H, Rouhani SJ, Ruddell A, et al. Lymph node-resident lymphatic endothelial cells mediate peripheral tolerance via Aire-independent direct antigen presentation. J Exp Med. 2010;207(4):681-8.
13. Lund AW, Duraes FV, Hirosue S, Raghavan VR, Nembrini C, Thomas SN, et al. VEGF-C Promotes Immune Tolerance in B16 Melanomas and Cross-Presentation of Tumor Antigen by Lymph Node Lymphatics. Cell Rep. 2012;1(3):191-9.
14. Tewalt EF, Cohen JN, Rouhani SJ, Guidi CJ, Qiao H, Fahl SP, et al. Lymphatic endothelial cells induce tolerance via PD-L1 and lack of costimulation leading to high-level PD-1 expression on CD8 T cells. Blood. 2012;120(24):4772-82.
15. Lund AW, Swartz MA. Role of lymphatic vessels in tumor immunity: passive conduits or active participants? J Mammary Gland Biol Neoplasia. 2010;15(3):341-52.
16. Rouhani SJ, Eccles JD, Tewalt EF, Engelhard VH. Regulation of T-cell Tolerance by Lymphatic Endothelial Cells. J Clin Cell Immunol. 2014;5:pli: 1000242.
17. Kowala MC, Schoefl GI. The popliteal lymph node of the mouse: internal architecture, vascular distribution and lymphatic supply. J Anat. 1986;148:25-46.
18. Harrell MI, Iritani BM, Ruddell A. Tumor-induced sentinel lymph node lymphangiogenesis and increased lymph flow precede melanoma metastasis. American Journal of Pathology. 2007;170(2):774-86.
19. Qian CN, Berghuis B, Tsarfaty G, Bruch M, Kort EJ, Ditlev J, et al. Preparing the "soil": the primary tumor induces vasculature reorganization in the sentinel lymph node before the arrival of metastatic cancer cells. Cancer Research. 2006;66(21):10365-76.
20. Garmy-Susini B, Avraamides CJ, Desgrosellier JS, Schmid MC, Foubert P, Ellies LG, et al. PI3Kalpha activates integrin alpha4beta1 to establish a metastatic niche in lymph nodes. Proc Natl Acad Sci U S A. 2013;110(22):9042-7.
21. Ruddell A, Kelly-Spratt KS, Furuya M, Parghi SS, Kemp CJ. p19/Arf and p53 suppress sentinel lymph node lymphangiogenesis and carcinoma metastasis. Oncogene. 2008;27:3145-55.
22. Ruddell A, Mezquita P, Brandvold KA, Farr A, Iritani BM. B lymphocyte-specific c-Myc expression stimulates early and functional expansion of the vasculature and lymphatics during lymphomagenesis. American Journal of Pathology. 2003;163:2233-45.
23. Ruddell A, Harrell MI, Furuya M, Kirschbaum SB, Iritani BM. B lymphocytes promote lymphogenous metastasis of lymphoma and melanoma. Neoplasia. 2011;13(8):748-57.
24. Hirakawa S, Kodama S, Kunstfeld R, Kajiya K, Brown LF, Detmar M. VEGF-A induces tumor and sentinel lymph node lymphangiogenesis and promotes lymphatic metastasis. J Exp Med. 2005;201:1089-99.
25. Hirakawa S, Brown LF, Kodama S, Paavonen K, Alitalo K, Detmar M. VEGF-C-induced lymphangiogenesis in

sentinel lymph nodes promotes tumor metastasis to distant sites. Blood. 2007;109:1010-7.
26. Fletcher AL, Lukacs-Kornek V, Reynoso ED, Pinner SE, Bellemare-Pelletier A, Curry MS, et al. Lymph node fibroblastic reticular cells directly present peripheral tissue antigen under steady-state and inflammatory conditions. J Exp Med. 2010;207(4):689-97.
27. Tewalt EF, Cohen JN, Rouhani SJ, Engelhard VH. Lymphatic endothelial cells - key players in regulation of tolerance and immunity. Front Immunol. 2012;3:305.
28. Hirosue S, Vokali E, Raghavan VR, Rincon-Restrepo M, Lund AW, Corthesy-Henrioud P, et al. Steady-state antigen scavenging, cross-presentation, and CD8+ T cell priming: a new role for lymphatic endothelial cells. J Immunol. 2014;192(11):5002-11.
29. Dubrot J, Duraes FV, Potin L, Capotosti F, Brighouse D, Suter T, et al. Lymph node stromal cells acquire peptide-MHCII complexes from dendritic cells and induce antigen-specific CD4(+) T cell tolerance. J Exp Med. 2014;211(6):1153-66.
30. Yeo KP, Angeli V. Bidirectional Crosstalk between Lymphatic Endothelial Cell and T Cell and Its Implications in Tumor Immunity. Front Immunol. 2017;8:83.
31. Lukacs-Kornek V, Malhotra D, Fletcher AL, Acton SE, Elpek KG, Tayalia P, et al. Regulated release of nitric oxide by nonhematopoietic stroma controls expansion of the activated T cell pool in lymph nodes. Nat Immunol. 2011;12(11):1096-104.
32. Norder M, Gutierrez MG, Zicari S, Cervi E, Caruso A, Guzman CA. Lymph node-derived lymphatic endothelial cells express functional costimulatory molecules and impair dendritic cell-induced allogenic T-cell proliferation. FASEB J. 2012;26(7):2835-46.
33. Gretz JE, Kaldjian EP, Anderson AO, Shaw S. Sophisticated strategies for information encounter in the lymph node: the reticular network as a conduit of soluble information and a highway for cell traffic. J Immunol. 1996;157(2):495-9.
34. Katakai T, Hara T, Lee JH, Gonda H, Sugai M, Shimizu A. A novel reticular stromal structure in lymph node cortex: an immuno-platform for interactions among dendritic cells, T cells and B cells. Int Immunol. 2004;16(8):1133-42.
35. Malhotra D, Fletcher AL, Turley SJ. Stromal and hematopoietic cells in secondary lymphoid organs: partners in immunity. Immunol Rev. 2013;251(1):160-76.
36. Swartz MA. Immunomodulatory roles of lymphatic vessels in cancer progression. Cancer Immunol Res. 2014;2(8):701-7.
37. Kataru RP, Kim H, Jang C, Choi DK, Koh BI, Kim M, et al. T lymphocytes negatively regulate lymph node lymphatic vessel formation. Immunity. 2011;34(1):96-107.
38. Habenicht L, Albershardt T, Iritani B, Ruddell A. Distinct mechanisms of B and T lymphocyte accumulation generate tumor-draining lymph node hypertrophy. Oncoimmunology. 2016;5:1204505-24.
39. Adams RH, Alitalo K. Molecular regulation of angiogenesis and lymphangiogenesis. Nat Rev Mol Cell Biol. 2007;8(6):464-78.
40. Baldwin ME, Stacker SA, Achen MG. Molecular Control of Lymphangiogenesis. Bioessays. 2002;24:1030-40.
41. Ferrara N. Role of vascular endothelial growth factor in regulation of angiogenesis. In: Teicher BA, editor. Angiogenesis. Totowa: Humana Press, Inc.; 1997. p. 119-41.
42. Shrestha B, Hashiguchi T, Ito T, Miura N, Takenouchi K, Oyama Y, et al. B cell-derived vascular endothelial growth factor A promotes lymphangiogenesis and high endothelial venule expansion in lymph nodes. J Immunol. 2010;184(9):4819-26.
43. Lee AS, Kim DH, Lee JE, Jung YJ, Kang KP, Lee S, et al. Erythropoietin induces lymph node lymphangiogenesis and lymph node tumor metastasis. Cancer Res. 2011;71(13):4506-17.
44. Ogawa F, Amano H, Eshima K, Ito Y, Matsui Y, Hosono K, et al. Prostanoid induces premetastatic niche in regional lymph nodes. J Clin Invest. 2014;124(11):4882-94.
45. Furuya M, Kirschbaum SB, Paulovich A, Pauli BU, Zhang H, Alexander JS, et al. Lymphatic endothelial murine chloride channel calcium-activated 1 is a ligand for leukocyte LFA-1 and Mac-1. J Immunol. 2010;185(10):5769-77.
46. Jordan-Williams KL, Ramanujam N, Farr AG, Ruddell A. The Lymphatic Endothelial mCLCA1 Antibody Induces Proliferation and Growth of Lymph Node Lymphatic Sinuses. PLoS One. 2016;11(5):e0156079.
47. Sabin FR. The lymphatic system in human embryos, with a consideration of the morphology of the system as a whole. Am. J. Anat. 1909;9:43-91.
48. Drinker CK, Field ME, Ward HK. The filtering capacity of lymph nodes. J Exp Med. 1934;59(4):393-405.
49. Gretz JE, Norbury CC, Anderson AO, Proudfoot AE, Shaw S. Lymph-borne chemokines and other low molecular weight molecules reach high endothelial venules via specialized conduits while a functional barrier limits access to the lymphocyte microenvironments in lymph node cortex. J Exp Med. 2000;192:1425-40.
50. Ikomi F, Hanna GK, Schmid-Schonbein GW. Mechanism of colloidal particle uptake into the lymphatic system: basic study with percutaneous lymphography. Radiology. 1995;196(1):107-13.
51. Partridge SC, Kurland BF, Liu CL, Ho RJ, Ruddell A. Tumor-induced lymph node alterations detected by MRI lymphography using gadolinium nanoparticles. Sci Rep. 2015;5:15641-55.
52. Ravizzini G, Turkbey B, Barrett T, Kobayashi H, Choyke PL. Nanoparticles in sentinel lymph node mapping. Wiley Interdiscip Rev Nanomed Nanobiotechnol. 2009;1(6):610-23.
53. Rantakari P, Auvinen K, Jappinen N, Kapraali M, Valtonen J, Karikoski M, et al. The endothelial protein PLVAP in lymphatics controls the entry of lymphocytes and antigens into lymph nodes. Nat Immunol. 2015;16(4):386-96.
54. Roozendaal R, Mempel TR, Pitcher LA, Gonzalez SF, Verschoor A, Mebius RE, et al. Conduits mediate transport of low-molecular-weight antigen to lymph node follicles. Immunity. 2009;30(2):264-76.
55. Sixt M, Kanazawa N, Selg M, Samson T, Roos G, Reinhardt DP, et al. The conduit system transports soluble antigens from the afferent lymph to resident dendritic cells in the T cell area of the lymph node. Immunity. 2005;22(1):19-29.
56. Kwon S, Sevick-Muraca EM. Noninvasive Quantitative

Imaging of Lymph Function in Mice. Lymphatic Research and Biology. 2007;5:219-32.
57. Ogata F, Azuma R, Kikuchi M, Koshima I, Morimoto Y. Novel lymphography using indocyanine green dye for near-infrared fluorescence labeling. Ann Plast Surg. 2007;58(6):652-5.
58. Kobayashi H, Hama Y, Koyama Y, Barrett T, Regino C, Urano Y, et al. Simultaneous Multicolor Imaging of Five Different Lymphatic Basins Using Quantum Dots. Nano Lett. 2007;7(6):1711-6.
59. Ruehm S, Corot C, Debatin J. Interstitial MR lymphography with a conventional extracellular gadolinium-based agent: assessment in rabbits. Radiology. 2001;218:664-9.
60. Kobayashi H, Kawamoto S, Star RA, Waldmann TA, Tagaya Y, Brechbiel MW. Micro-magnetic resonance lymphangiography in mice using a novel dendrimer-based magnetic resonance imaging contrast agent. Cancer Res. 2003;63(2):271-6.
61. Mounzer R, Shkarin P, Papademetris X, Constable T, Ruddle NH, Fahmy TM. Dynamic imaging of lymphatic vessels and lymph nodes using a bimodal nanoparticulate contrast agent. Lymphat Res Biol. 2007;5(3):151-8.
62. McElroy M, Hayashi K, Garmy-Susini B, Kaushal S, Varner JA, Moossa AR, et al. Fluorescent LYVE-1 antibody to image dynamically lymphatic trafficking of cancer cells in vivo. J Surg Res. 2009;151(1):68-73.
63. Zhang F, Niu G, Lin X, Jacobson O, Ma Y, Eden HS, et al. Imaging tumor-induced sentinel lymph node lymphangiogenesis with LyP-1 peptide. Amino Acids. 2011.
64. Mumprecht V, Honer M, Vigl B, Proulx ST, Trachsel E, Kaspar M, et al. In vivo imaging of inflammation- and tumor-induced lymph node lymphangiogenesis by immuno-positron emission tomography. Cancer Res. 2010;70(21):8842-51.
65. Habal N, Giuliano AE, Morton DL. The use of sentinel lymphadenectomy to identify candidates for postoperative adjuvant therapy of melanoma and breast cancer. Semin Oncol. 2001;28(1):41-52.
66. Newman EA, Newman LA. Lymphatic mapping techniques and sentinel lymph node biopsy in breast cancer. Surg Clin North Am. 2007;87(2):353-64, viii.
67. Ruddell A, Kirschbaum SB, Ganti SN, Liu CL, Sun RR, Partridge SC. Tumor-induced alterations in lymph node lymph drainage identified by contrast-enhanced MRI. J Magn Reson Imaging. 2015;42:145-52.
68. Katakai T, Hara T, Sugai M, Gonda H, Shimizu A. Lymph node fibroblastic reticular cells construct the stromal reticulum via contact with lymphocytes. J Exp Med. 2004;200(6):783-95.
69. Harris AW, Pinkert CA, Crawford M, Langdon WY, Brinster RL, Adams JM. The Eμ-*c-myc* transgenic mouse. A model for high-incidence spontaneous lymphoma and leukemia of early B cells. Journal of Experimental Medicine. 1988;167(2):353-71.
70. Harrell MI, Iritani BM, Ruddell A. Lymph Node Mapping in the Mouse. J. Immunological Methods. 2008;332:170-4.
71. Grandori C, Eisenman RN. Myc target genes. Trends in Biochemical Sciences. 1997;22(5):177-81.
72. Mezquita P, Parghi SS, Brandvold KA, Ruddell A. Myc regulates VEGF production in B cells by stimulating initiation of VEGF mRNA translation. Oncogene. 2005;24(5):889-901.
73. Astarita JL, Cremasco V, Fu J, Darnell MC, Peck JR, Nieves-Bonilla JM, et al. The CLEC-2-podoplanin axis controls the contractility of fibroblastic reticular cells and lymph node microarchitecture. Nat Immunol. 2015;16(1):75-84.
74. Felten DL, Livnat S, Felten SY, Carlson SL, Bellinger DL, Yeh P. Sympathetic innervation of lymph nodes in mice. Brain Res Bull. 1984;13(6):693-9.
75. Thornbury KD, McHale NG, Allen JM, Hughes G. Nerve-mediated contractions of sheep mesenteric lymph node capsules. J Physiology (Lond). 1990;422:513-22.
76. Hughes GA, Allen JM. Neural modulation of bovine mesenteric lymph node contraction. Exp Physiol. 1993;78(5):663-74.
77. Gogineni A, Caunt M, Crow A, Lee CV, Fuh G, van Bruggen N, et al. Inhibition of VEGF-C modulates distal lymphatic remodeling and secondary metastasis. PLoS One. 2013;8(7):e68755.
78. Karnezis T, Shayan R, Caesar C, Roufail S, Harris NC, Ardipradja K, et al. VEGF-D promotes tumor metastasis by regulating prostaglandins produced by the collecting lymphatic endothelium. Cancer Cell. 2012;21(2):181-95.
79. Kobayashi H, Kawamoto S, Sakai Y, Choyke PL, Star RA, Brechbiel MW, et al. Lymphatic drainage imaging of breast cancer in mice by micro-magnetic resonance lymphangiography using a nano-size paramagnetic contrast agent. J Natl Cancer Inst. 2004;96(9):703-8.
80. Tsuda N, Tsuji T, Kato N. Interstitial magnetic resonance lymphography using gadolinium-ethoxybenzyl-diethylenetriamine pentaacetic acid in rabbits with lymph node metastasis. Invest Radiol. 2005;40(5):306-12.
81. Ruddell A, Harrell M, Minoshima S, Maravilla K, Iritani B, White S, and , et al. Dynamic contrast-enhanced magnetic resonance imaging of tumor-induced lymph flow. Neoplasia. 2008;10:706-13.
82. Proulx ST, Ma Q, Andina D, Leroux JC, Detmar M. Quantitative measurement of lymphatic function in mice by noninvasive near-infrared imaging of a peripheral vein. JCI Insight. 2017;2(1):e90861.
83. Ji RC. Lymph Nodes and Cancer Metastasis: New Perspectives on the Role of Intranodal Lymphatic Sinuses. Int J Mol Sci. 2016;18(1).
84. Ruddell A, Croft A, Kelly-Spratt K, Furuya M, Kemp CJ. Tumors induce coordinate growth of artery, vein, and lymphatic vessel triads. BMC Cancer. 2014;14:354.
85. Nathanson SD, Mahan M. Sentinel Lymph Node Pressure in Breast Cancer. Ann Surg Oncol. 2011.
86. Padera TP, Kadambi A, di Tomaso E, Carreira CM, Brown EB, Boucher Y, et al. Lymphatic metastasis in the absence of functional intratumor lymphatics. Science. 2002;296(5574):1883-6.
87. Kwon S, Agollah GD, Wu G, Chan W, Sevick-Muraca EM. Direct visualization of changes of lymphatic function and drainage pathways in lymph node metastasis of B16F10 melanoma using near-infrared fluorescence imaging. Biomed Opt Express. 2013;4(6):967-77.
88. Proulx ST, Luciani P, Christiansen A, Karaman S, Blum KS, Rinderknecht M, et al. Use of a PEG-conjugated bright

near-infrared dye for functional imaging of rerouting of tumor lymphatic drainage after sentinel lymph node metastasis. Biomaterials. 2013;34(21):5128-37.
89. Scoggins CR, Martin RC, Ross MI, Edwards MJ, Reintgen DS, Urist MM, et al. Factors associated with false-negative sentinel lymph node biopsy in melanoma patients. Ann Surg Oncol. 2010;17(3):709-17.
90. Spillane AJ, Brennan ME. Accuracy of sentinel lymph node biopsy in large and multifocal/multicentric breast carcinoma--a systematic review. Eur J Surg Oncol. 2011;37(5):371-85.
91. Treuting P, Dintzis S. Comparative Anatomy and Histology: A Mouse and Human Atlas. Waltham, MA USA: Academic Press; 2012.
92. Forkert PG, Thliveris JA, Bertalanffy FD. Structure of sinuses in the human lymph node. Cell Tissue Res. 1977;183(1):115-30.
93. Kadowaki I, Ichinohasama R, Harigae H, Ishizawa K, Okitsu Y, Kameoka J, et al. Accelerated lymphangiogenesis in malignant lymphoma: possible role of VEGF-A and VEGF-C. British Journal of Haematology. 2005;130:869-77.
94. Maza S, Valencia R, Geworski L, Sandrock D, Zander A, Audring H, et al. Influence of fast lymphatic drainage on metastatic spread in cutaneous malignant melanoma: a prospective feasibility study. Eur J Nucl Med Mol Imaging. 2003;30(4):538-44.
95. Fujiwara M, Sawada M, Kasuya A, Matsushita Y, Yamada M, Fukamizu H, et al. Measurement of cutaneous lymphatic flow rates in patients with skin cancer: area extraction method. J Dermatol. 2014;41(6):498-504.
96. Swartz MA, Lund AW. Lymphatic and interstitial flow in the tumour microenvironment: linking mechanobiology with immunity. Nat Rev Cancer. 2012;12(3):210-9.
97. Jeanbart L, Ballester M, de Titta A, Corthesy P, Romero P, Hubbell JA, et al. Enhancing efficacy of anticancer vaccines by targeted delivery to tumor-draining lymph nodes. Cancer Immunol Res. 2014;2(5):436-47.
98. Thomas SN, Vokali E, Lund AW, Hubbell JA, Swartz MA. Targeting the tumor-draining lymph node with adjuvanted nanoparticles reshapes the anti-tumor immune response. Biomaterials. 2014;35(2):814-24.
99. Herborn CU, Lauenstein TC, Vogt FM, Lauffer RB, Debatin JF, Ruehm SG. Interstitial MR lymphography with MS-325: characterization of normal and tumor-invaded lymph nodes in a rabbit model. AJR Am J Roentgenol. 2002;179(6):1567-72.
100. Van den Eynden GG, Van der Auwera I, Van Laere SJ, Huygelen V, Colpaert CG, van Dam P, et al. Induction of lymphangiogenesis in and around axillary lymph node metastases of patients with breast cancer. Br J Cancer. 2006;95(10):1362-6.
101. Van den Eynden GG, Vandenberghe MK, van Dam PJ, Colpaert CG, van Dam P, Dirix LY, et al. Increased sentinel lymph node lymphangiogenesis is associated with non-sentinel axillary lymph node involvement in breast cancer patients with a positive sentinel node. Clin Cancer Res. 2007;13(18 Pt 1):5391-7.
102. Pastushenko I, Van den Eynden GG, Vicente-Arregui S, Prieto-Torres L, Alvarez-Alegret R, Querol I, et al. Increased Angiogenesis and Lymphangiogenesis in Metastatic Sentinel Lymph Nodes Is Associated With Nonsentinel Lymph Node Involvement and Distant Metastasis in Patients With Melanoma. Am J Dermatopathol. 2016;38(5):338-46.
103. Ishii H, Chikamatsu K, Sakakura K, Miyata M, Furuya N, Masuyama K. Primary tumor induces sentinel lymph node lymphangiogenesis in oral squamous cell carcinoma. Oral Oncol. 2010;46(5):373-8.
104. Hirota K, Wakisaka N, Sawada-Kitamura S, Kondo S, Endo K, Tsuji A, et al. Lymphangiogenesis in regional lymph nodes predicts nodal recurrence in pathological N0 squamous cell carcinoma of the tongue. Histopathology. 2012;61(6):1065-71.
105. Jakob C, Aust DE, Liebscher B, Baretton GB, Datta K, Muders MH. Lymphangiogenesis in regional lymph nodes is an independent prognostic marker in rectal cancer patients after neoadjuvant treatment. PLoS One. 2011;6(11):e27402.